Numerical simulation of deflagration to detonation transition with wall cooling effect in ethylene-air mixture

Min-cheol Gwak, Ki-hong Kim, and Jack J. Yoh *
School of Mechanical and Aerospace Engineering
Seoul National University, Seoul, Korea 151-742

1 Introduction

The combustion phenomenon of present study concerns two modes of burning that are deflagration and detonation. Here, deflagration is a subsonic mode of combustion at relatively lower pressure, while detonation is a supersonic mode of combustion at relatively higher pressure. The characteristic modes of two flames are well understood by the theoretical Rankine-Hugoniot curve. DDT is an extremely complex process involving deflagrations, shocks and shock reflections, boundary layers and all of their interactions with each other. The mechanism of DDT occurrence is not clear in experiments, and it varies from case to case. However the principle of DDT mechanism is that a flame needs acceleration process for DDT to occur. So the study of FA is a pre-requisite for understanding the DDT process [1-4]. The acceleration process includes i) development of turbulent flow condition, ii) hot spot generation, and iii) flame instabilities or Richtmyer-Meshkov (RM) instability, which arises when a shock wave interacts with interface separating the two fluids of different density, reactant and product in combustion [5]. These sub-processes become fully coupled and their interactions with each other are the key factor in understanding the basic mechanism. These processes increase flame surface area, which naturally increases the chemical reaction rate, leading to a high energy release. Specially, the interaction of pressure waves with flame front between reactant and product is an important mechanism that can lead to flame acceleration, fast deflagration, and DDT in mixtures [4]. In this paper, we report a fully resolved two-dimensional simulation of shock-flame interactions and the effect of wall cooling through a comparison between adiabatic and constant temperature wall conditions.

2 Formulation

2.1 Governing equations

To simulate DDT process, we solve the multidimensional, time-dependent, reactive compressible Navier-Stokes equations (conservation laws of mass, x-axis momentum, y-axis momentum, energy, and species) with equation of state of an ideal gas in a 2D coordinate. We include models for viscosity, thermal conduction, molecular diffusion, and chemical reaction. One-step chemical reaction in the form of Arrhenius rate law $A\rho Y_i \exp(-E_a / RT)$ is used. And we assume that kinematic viscosity, diffusion, and heat conduction coefficients are dependent on temperature and density[6].

Correspondence to: jjyoh@snu.ac.kr

The convective effects are handled by the 4th-order Convex ENO scheme for spatial discretization, and 3rd-order Runge-Kutta (RK) integration is used for time [7]. Viscous, heat conduction, and mass diffusion fluxes are evaluated using the second-order finite difference method. In the model, subgrid model of turbulent-energy dissipation is not considered because the effect of RM instability is dominant (roughly twice as large as the Kolmogorov decay) in contribution to the characteristic scale of eddy vortices [1].

In order to fully resolve the reaction zone thickness, we require that the mesh size be 0.1 mm. We performed 3 different grid refinements (0.2, 0.1, and 0.05mm) to meet grid independence and determined 0.1mm to be optimal. This resolution corresponds to approximately 10 computational cells in laminar flame thickness of about 0.96 mm.

2.2 Simulation setup: initial and boundary conditions

We use the stoichiometric ethylene-air mixture for the flame and shock interaction study. The initial temperature, pressure, density, mass fraction of reactant, gamma and molecular weight are 293K, 1.33×10^{4}J/m^{3}, 1.58×10^{-1}kg/m^{3}, 1, 1.15, and 29×10^{-3}kg/mol, respectively. For the chemical reaction parameters, pre-exponential factor, activation energy, and chemical energy release are 3.2×10^{8}m^{3}/kg·s, $35.351RT_0$, and $48.824RT_0/M$, respectively.

We model (see Fig. 1) a section of the shock tube of 220 mm by 38 mm, using a zero gradient inflow condition on the left, wall reflection on the right, symmetry on the upper boundary, and no slip wall on the lower wall. In particular, two different wall conditions being adiabactic and constant temperature wall condition for considering the wall cooling effect are considered. In Fig. 1, the incident shock of specified strength [9] is initially placed 63 mm from the inlet. Two gages are located 55 mm (labeled 1) and at 185 mm (labeled 2) for measuring the pressure variation.

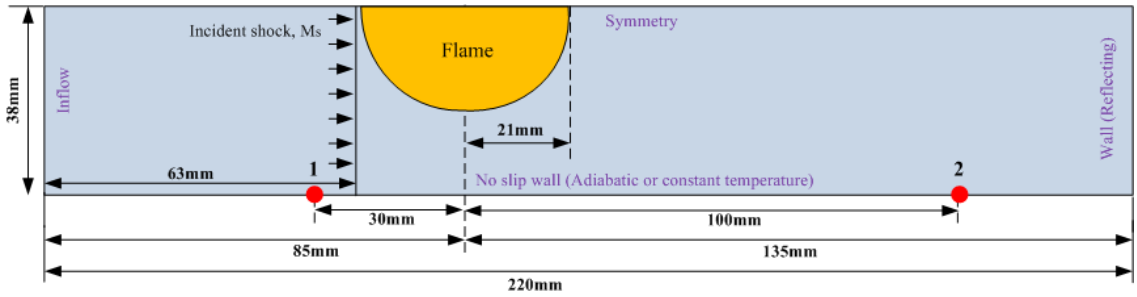

Figure 1. Schematic of numerical setup

A flame is initially located at 85 mm from the inlet with its initial diameter 42 mm. The flame thickness is assumed a discontinuity, which separates the adiabatic flame condition (flame temperature T_b = 2625 K, density $\rho_b = 1.77 \times 10^{-2}$kg/m^{3}) from the surround.

3 Results and discussion

We perform DDT simulation of stoichiometric ethylene-air mixture using pre-mentioned governing equations, initial conditions, and boundary conditions.

3.1 DDT induced by shock and flame interaction

Figure 2 shows the time sequence of temperature fields under Ma=1.9 incident shock interacting with an ethylene-air flame in the adiabatic wall condition. Time 0 ms shows the initial flame located 85 mm

from the inlet. With time, the shock and flame interaction begins where flame becomes distorted following the Richtmyer-Meshkov (RM) instability. The transmitted shock through the flame moves downward and reflects off the wall at times 0.2 and 0.3 milliseconds.

The lambda-shock structure is then formed on the bottom wall after the wall reflection in Fig. 2(c). This structure is composed of a thin boundary layer, bifurcated foot, and a tail shock, and it is generated by the reflected shock that interacts with the existing boundary layer[10]. Flame instability creates a large funnel of unburned gas that penetrates the burned region and is well observed at time 0.4ms. Through growth of this funnel, the energy-release rate is increased in the unburned gas due to increasing flame surface, and the lambda shock is strengthened. In Fig. 2(e)-(f), lambda-shock structure continues to develop with stronger recirculation zone behind.

The velocity of the flame tip is faster than the general laminar flame velocity, roughly in the same order as the oblique shock velocity along the bottom wall. This flame approaches the oblique shock front and quickly spreads into the unburned gas due to existence of rotational zone (see Fig. 3) behind the lambda-shock structure. Through this process, flame surface is enlarged, and energy-release rate increases until the lambda-shock structure reaches the symmetry plane on the upper boundary. Before 0.64 milliseconds, hot spot is generated by the interaction between multi-shock and flame in the upper part of the flame as a stretched funnel. Then the flame spreads in all directions at time onward after triggering the detonation.

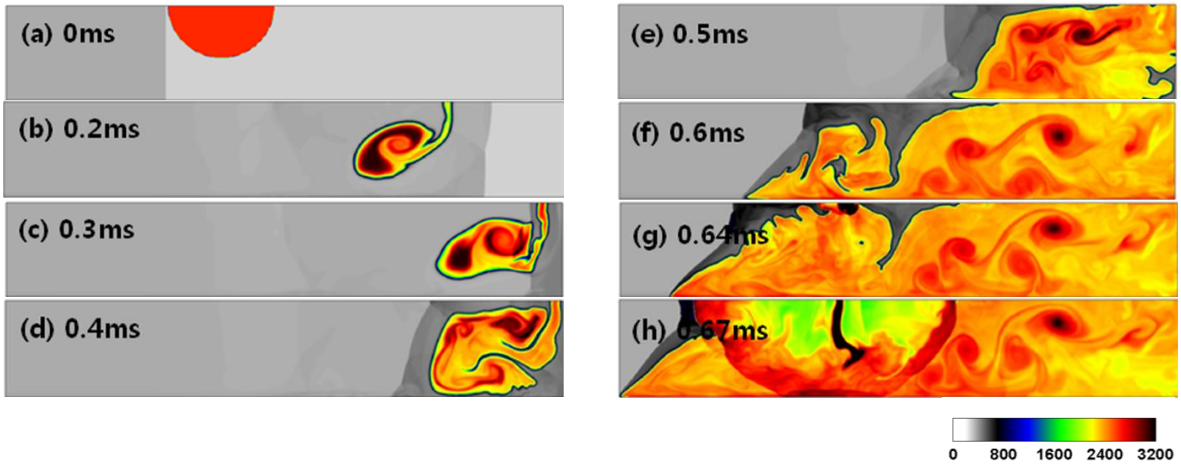

Figure 2. Time sequence of temperature field (Kelvin) under Ma=1.9 incident shock interacting with an ethylene-air flame in adiabatic wall condition

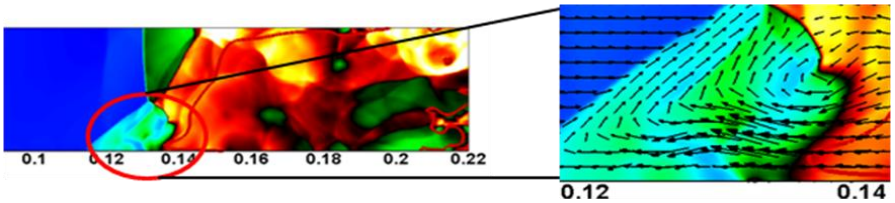

(a) Front tip of flame (red line) runs into the back side of lambda shock

(b) Zoom-in flame tip in (a)

Figure 3. Pressure contour (Pa) and velocity vector shown in adiabatic wall case at 0.495ms

Figure 4 shows the pressure histories at two gages in Fig. 1. Label-① shows the incident shock wave (pressure: 0.05MPa, density: 0.4825kg/m^3, temperature: 363K) propagating to the right. Label-② in

both figures marks the left running strange wave that is a multi-reflection wave strengthened by merging of the reflection waves shown in Fig. 3(a). The propagation velocity of the flame is approximately 1500 m/s, and the increasing pressure ratio is roughly 10 times reaching 0.5MPa. Finally, label-③ shows pressure peak 0.84 MPa of a propagating detonation, which is about twice the pressure of the strange wave marked ②.

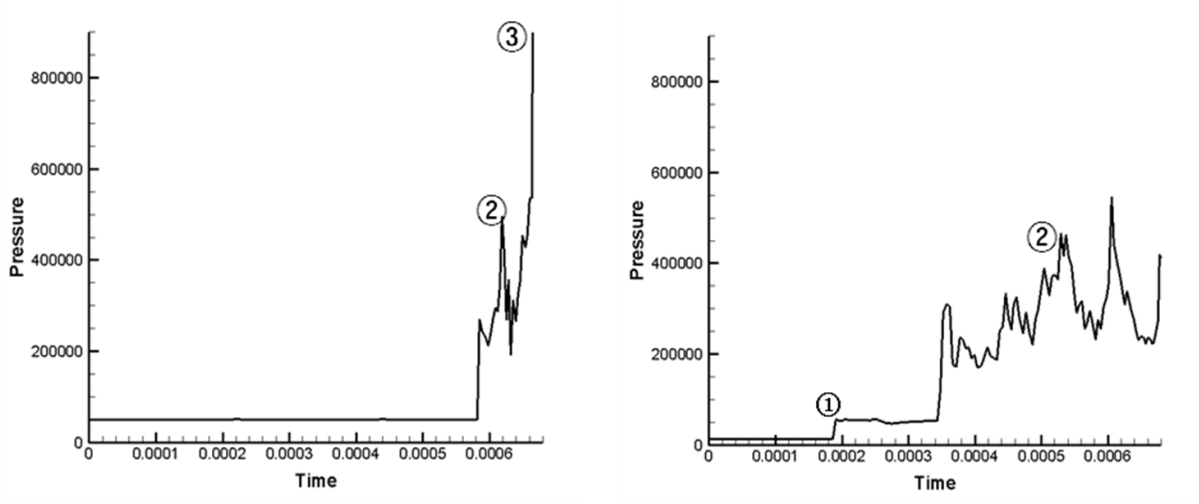

(a) Gage 1 (b) Gage 2

Figure 4. Calculated pressure histories along the tube

3.2 Comparison of adiabatic and constant temperature wall conditions

Figure 5 shows the time sequence of temperature fields under Ma=1.9 incident shock interacting with an ethylene-air flame under constant temperature (293 K) and no slip wall conditions.

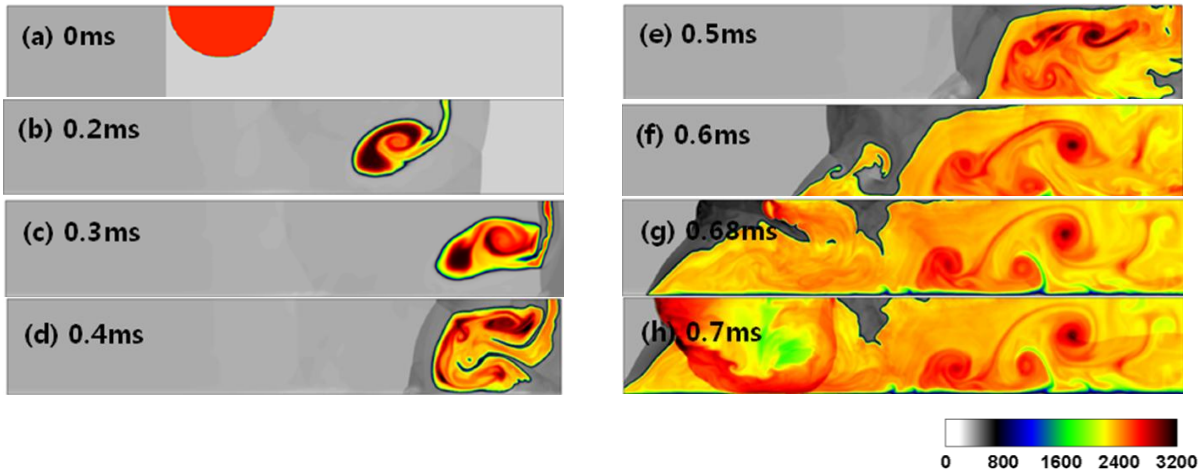

Figure 5. Time sequence of temperature field (Kelvin) under Ma=1.9 incident shock interacting with an ethylene-air flame in constant temperature (293K) wall condition

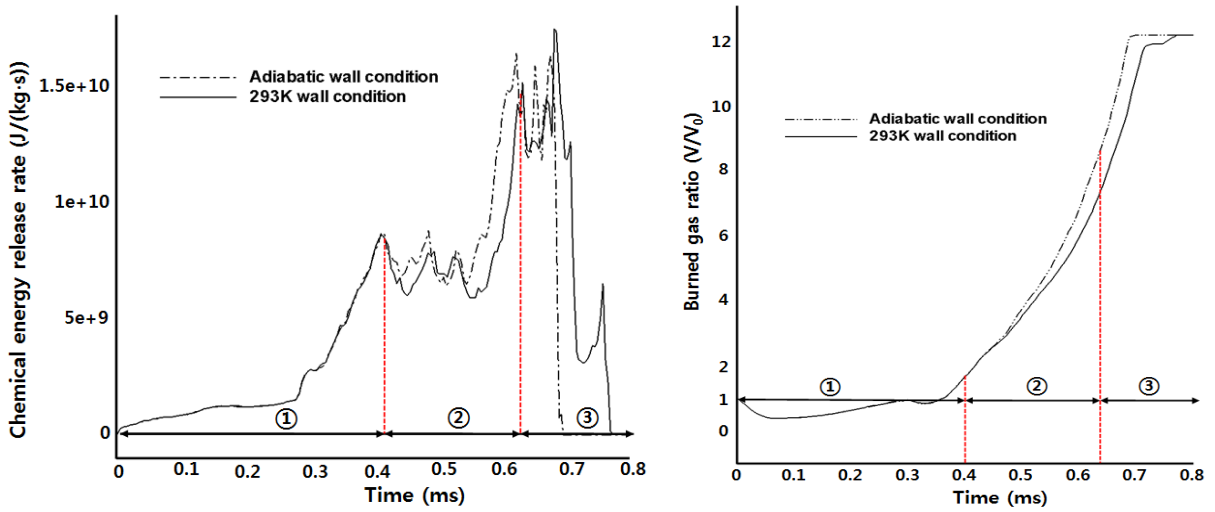

(a) (b)

Figure 6. Time histories of (a) chemical heat release rate and (b) burned gas ratio for two different wall conditions

Flame propagation characteristic is similar overall in both adiabatic and constant temperature wall conditions. However, formation of lambda-shock structure and area of flame surface are noted quite different. Figure 6 shows the time histories in chemical energy release rate (*de/dt*, unit: J/kg·s) and the burned gas ratio (total burned gas versus initial burned gas, $0 \le V/V_0 \le 12$) at two different wall conditions. Before appearing of lambda-shock structure, the two cases are identical in region 1. The flame expansion of constant wall condition is delayed due to weakened rotational flow behind the lambda-shock structure shown in region 2. As a result, detonation triggering time is delayed and it is 0.68 ms as opposed to 0.64 ms in the case of adiabatic wall condition (see region 3).

On going effort on flame acceleration in an enclosed volume includes multi-bend tube simulation. Figure 7 shows both strange wave acceleration and development of DDT in the smoothed duct flow containing the ethylene-air mixture. Incident shock strength of Ma=2.7 is used to initiate DDT in the present simulation.

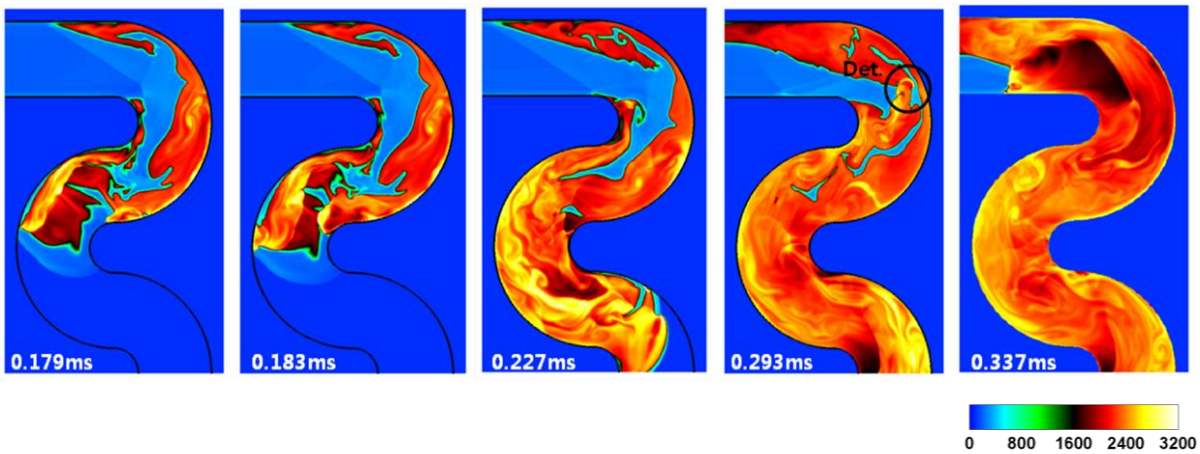

Figure 7. Time sequence of temperature field under Ma=2.7 incident shock interacting with an ethylene-air flame in multi-bend pipe (unit:K)

4 Conclusion

We confirm that strong interaction of shock and flame is an important factor in creating the deflagration to detonation transition in ethylene-air mixture in a closed tube. The details of flame acceleration of ethylene-air mixture are presented through the numerical simulation outlined in this work. The RM instability and rotational zone behind the lambda-shock structure are mainly responsible for the flame stretch through pressure fluctuations in the shock-flame interaction as hot spots are being seeded in the unburned region. Furthermore, constant temperature wall condition delayed detonation triggering time when compared to adiabatic wall condition due to wall cooling effect.

Acknowledgment

Authors would like to thank the financial support from the Hyundai Motor Group and ADD through the Institute of Advanced Aerospace Technology and ERI at Seoul National University

References

[1] Khokhlov AM, Oran ES, Thomas GO. (1999). Numerical simulation of deflagration-to-detonation transition: The role of shock-flame interactions in turbulent flames. Combust. Flame. 117: 323.

[2] Oran ES, Khokhlov AM. (1999). Deflagration, hot spots, and the transition to detonation. Phil. Trans. R. Soc. Lond., 357: 3539.

[3] Ciccarelli G, Dorofeev S. (2008). Flame acceleration and transition to detonation in ducts. Prog. Energy. Combust. Sci. 34: 499.

[4] Lee JHS, Moen IO. (1980). The mechanism of transition from deflagration to detonation in vapor cloud explosions. Prog. Energy Combust. Sci. 6: 359.

[5] Brouillette M. (2002). The Richtmyer-Meshkov instability. Annu. Rev. Fluid Mech. 34: 445.

[6] Khokhlov AM, Oran ES, Chtchelkanova AY. (1999). Interaction of a shock with sinusoidally perturbed flame. Combust. Flame. 117: 99.

[7] Liu XD, Osher S. (1998). Convex ENO high order multi-dimensional schemes without field by field decomposition or staggered grids. J. Comput. Physics. 141: 1.

[8] Thomas G, Bambrey R, Brown C. (2001). Experimental observations of flame acceleration and transition to detonation following shock-flame interaction. Combust. Theory Modelling. 5: 573.

[9] James EAJ. (2006). Gas dynamics, 3rd ed. Pearson Prentice Hall.

[10] Mark H. (1958). The interaction of a reflected shock wave with the boundary layer in a shock tube. NACA TM 1418